SPARC/EBD-07/005

06 Settembre 2007

NoLFiPS: Non Linear Fit of Phase Spaces

Andrea R. Rossi *

INFN - MI

Abstract

In this note, we show how a non linear fitting of the phase spaces reconstructed from SPARC emittance-meter data, can be used to perform an analysis of the beam chromatic components after the focusing solenoid field. This implies a first step toward a beam tomography, retrieving some pieces of informations on the bunch longitudinal phase space from projected transverse phase spaces.

* andrea.rossi@mi.infn.it

1. INTRODUCTION

The quality of a beam produced by an accelerating structure such as SPARC gun, is estimated by the use of transverse emittance, which is the r.m.s. area of an ellipse whose perimeter encloses most (in an r.m.s. way) of the beam trace in a transverse phase space (PS). From a theoretical point of view the ellipse is justified by the fact that, if a bunch experiences only linear transverse forces, it is exactly the shape assumed in the transverse PS by the charge density; in fact, under certain conditions [1], the areas of the geometrical ellipse and of the r.m.s. ellipse (i.e. the emittance), are proportional.

In real beams the transverse PS trace is seldom elliptical. Nonlinearities in the line optical elements produce a distortion of the theoretical shape, giving it a typical S shape, while dynamical effects can produce multiple, concentrical ellipses. We will focus on the former phenomena, where the single ellipse is divided in two or more ellipses with different cinematical behaviors: the interplay of different ellipses orientation could produce the double minima effect [2]. Usually two ellipses are clearly visible with one ellipse representing most of the beam charge ($\gtrsim 90\%$), which we will call it main beam (MB), while the other ellipse holds much less charge and will be called secondary beam (SB). Multiple ellipses are due mainly to two sources: *cross over* and chromatic (energy spread) affects. In a focusing apparatus, if we describe the beam in cylindrical coordinates, the cross over manifests when a particle's radial momentum doesn't change its sign at the beam waist, meaning that it crosses the $r = 0$ coordinates, so the beam behaves like a nonlaminar fluid; this is due to low density charges along the longitudinal direction (such as the head and queue of gaussian beams) and/or strong focusing forces. Energy spread effects are due to the different focusing strenght experienced by particles with different energies (like the chromatic aberration of spherical lenses) in the longitudinal directions. In this situation the radial momenum "bounces" off the z axis and the beam behaves like a laminar fluid.

Thanks to the different particles behavior, the two sources can be distinguished by inspection of the transverse PSs taken at different z coordinates (z-scan) [3]. Since both effects are due to beam properties with different values along its length, separating different beam components in the transverse PSs is equivalent to performing a tomography of the beam, retrieving longitudinal informations from projected measurements. Furthermore, isolating the MB component, allows to better estimate the beam emittance, since the r.m.s. ellipse area is enlarged by the presence of non coaxial secondary components.

To this end, we implemented a procedure that performs a non linear fitting of the transverse PSs, enabling us to separate the different beam components, evaluate their charge and computing their emittance separately. Our results have been compared with other algorithms used to calculate emittance [4–6].

2. FITTING FUNCTION

Probably the most important ingredient in a method like NoLFiPS is the fitting function. By a visual inspection of the reconstructed transverse PSs and theoretical considerations, a couple of reasonable features can be highlighted; first, if we disregard nonlinear effects showing up at the border regions from the origin of coordinates, the PSs should be nearly central symmetric, ideally elliptic in shape, or a sum of ellipses with a common center. Second, the PS density distribution seems either to decrease linearly from its maximum or appears as a sum of two parabola like shapes, one on top of the other. Keeping in mind that, from a theoretical point of view, the density distribution should drop to zero faster than a gaussian for a transversally uniform charge distribution, we decided to use a fit function of this form:

$$f(\theta,\phi,\Sigma,\sigma) = Q_1^2\, e^{-r(\theta,\Sigma_1)-r^2(\theta,\Sigma_2)-r^4(\theta,\Sigma_4)} + Q_2^2\, e^{-r(\phi,\sigma_1)-r^2(\phi,\sigma_2)-r^4(\phi,\sigma_4)}\,, \tag{1}$$

where

$$r(\alpha,s) = \sqrt{\left(\frac{(x-x_0)\cos\alpha}{s_x} + \frac{(x'-x'_0)\sin\alpha}{s_{x'}}\right)^2 + \left(\frac{(x'-x'_0)\cos\alpha}{s_x} - \frac{(x-x_0)\sin\alpha}{s_{x'}}\right)^2}\,. \tag{2}$$

A total of 18 parameters must be fitted using the least squares method. This function, being the sum of two exponentials with different orientations, can cope with the different dynamic obeyed by the core portion of the bunch and the head-tail areas, yielding some informations on the charge content of both portions.

3. STARTING PARAMETERS

NoLFiPS performs a nonlinear fit of the PS density distribution. The results of such kind of fittings heavily depend on the initial parameters' values, both in convergence speed and final correspondence between the fit and the experimental data. A standard procedure to insert sound starting values, for the main beam portion, has been elaborated.

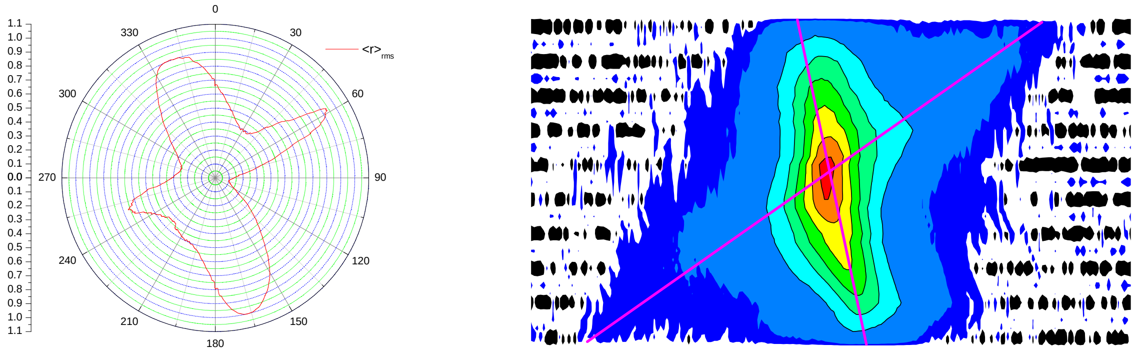

FIG. I: The r.m.s. profile of the PS normalized to one (left) and the two ellipses' main axes displayed on the charge distribution (right). Notice that the two pictures have different aspect ratios, so the angles don't seem to match.

First of all, the radial r.m.s. profile of the PS is calculated by using ad *ad hoc* code. In doing this it is important to chose the appropriate rotation point that can be either the maximum of charge distribution or its center of mass: in an ideal PS they coincide, while in experimental data it usually better to use the former, since the charge distribution can feature an off symmetry maximum when the two ellipses lay along the same direction; the result of such operation is shown in FIG. I on the left. From the profile it is possible to obtain one or two lines, corresponding to the major axis (axes) of the ellipse(s) (FIG: I right). Then the charge distribution

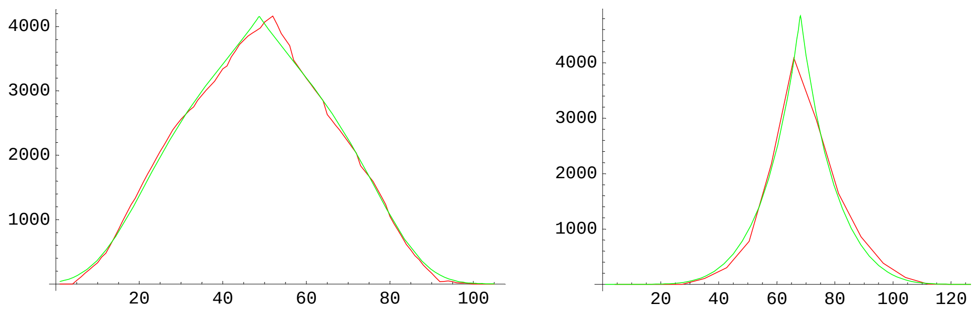

FIG. II: Profiles of the phase space distributions along the two symmetry axes of the main beam ellipse: experimental data (red) and fit function (green). The x axis labels are matrix related rows and columns numbers.

is evaluate along the line corresponding to the main beam portion and its normal intersecting in the center of mass, thus yielding two slices of the PS; the line associated to the secondary beam is not used in the following at present, except for its direction whose fed to NoLFiPS as the direction ϕ of the secondary beam. The slices are fitted with the one dimensional, one exponential version of the fitting function (1):

$$f(z,\alpha) = Q_1^2\, e^{-\frac{|z-z_0|}{\alpha_1} - \left(\frac{z-z_0}{\alpha_2}\right)^2 - \left(\frac{z-z_0}{\alpha_4}\right)^4} . \tag{3}$$

The results are two orthogonal profiles, shown in FIG. II, whose fitted parameters are used as starting values for the complete two dimensional fit.

The starting values returned by the above procedure, yield a fitting function for the main beam fraction that is displayed in FIG. III; the starting values for the secondary beam, except for the direction, are inserted by hand. This arbitrary choice has been found to be acceptable, since the fixing of the main beam starting values has proved to be enough in order to assure a good convergence of the fitting.

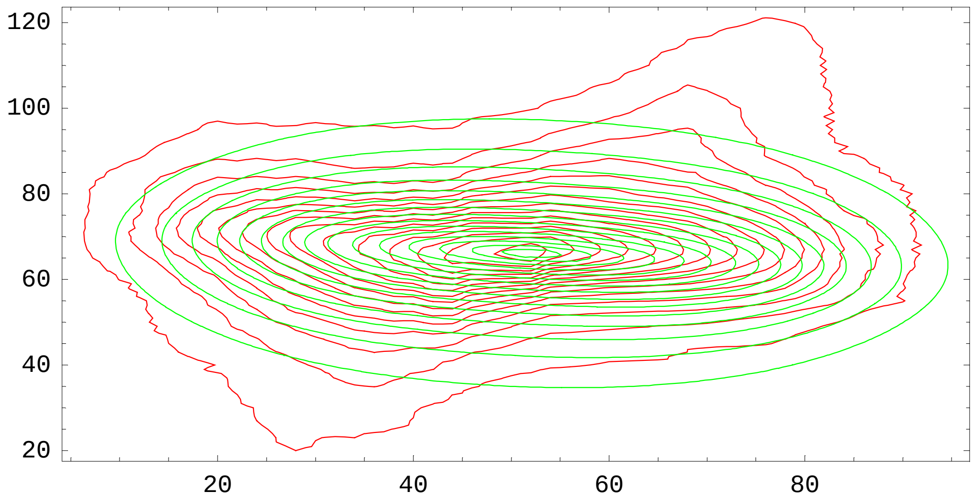

FIG. III: The starting PS profile generated by the procedure described in Section 3 (red) and experimental data (green). The axes labels are matrix columns and rows numbers.

There is, at present, one obvious situation in which the procedure fails to operate, namely when the two ellipses axes are orthogonal: this requires the intervention of an operator.

4. SCAN RESULTS

We applied NoLFiPS to the scan results of the runs with a flat top bunch, taken on 26/11/2006. In the following FIGs. IV - VIII some examples of reconstructed phase spaces are shown: the false colors patterns are not directly confrontable between any two figures, since the values' span is not the same; dark blue areas are either very high charge density values, if surrounded by red halos, or mildly negative values if surrounding green-light blue regions; in each figure, the axes labels are columns and rows numbers, while the six pictures in each page are as follows:

B1 is the fitted complete phase space;

B2 is the fitted main beam, *i.e.* equation (1) with $Q_2 = 0$;

B3 is the fitted secondary beam, *i.e.* equation (1) with $Q_1 = 0$;

A1 is the experimental phase space;

A2 is the “experimental” main beam, obtained by computing A1-B3;

A3 is the “experimental” secondary beam, obtained by computing A1-B2.

It is worth to note that NoLFiPS works remarkably well even when the reconstructed experimental PSs have disconnected or displaced parts, such as in FIG. IV and FIG. VIII. More, when part of the charge density has been cut during the measuring process, NoLFiPS can reconstruct the missing portion, at least in part (see FIG. V). As could be expected, some problems show up when the assumptions made in Section 2 do not hold: it is clear from pictures B3 of FIGs. IV and V that the experimental results show a significantly non central symmetric charge distribution; nevertheless the core portion, in the transverse PS, usually looks well fitted.

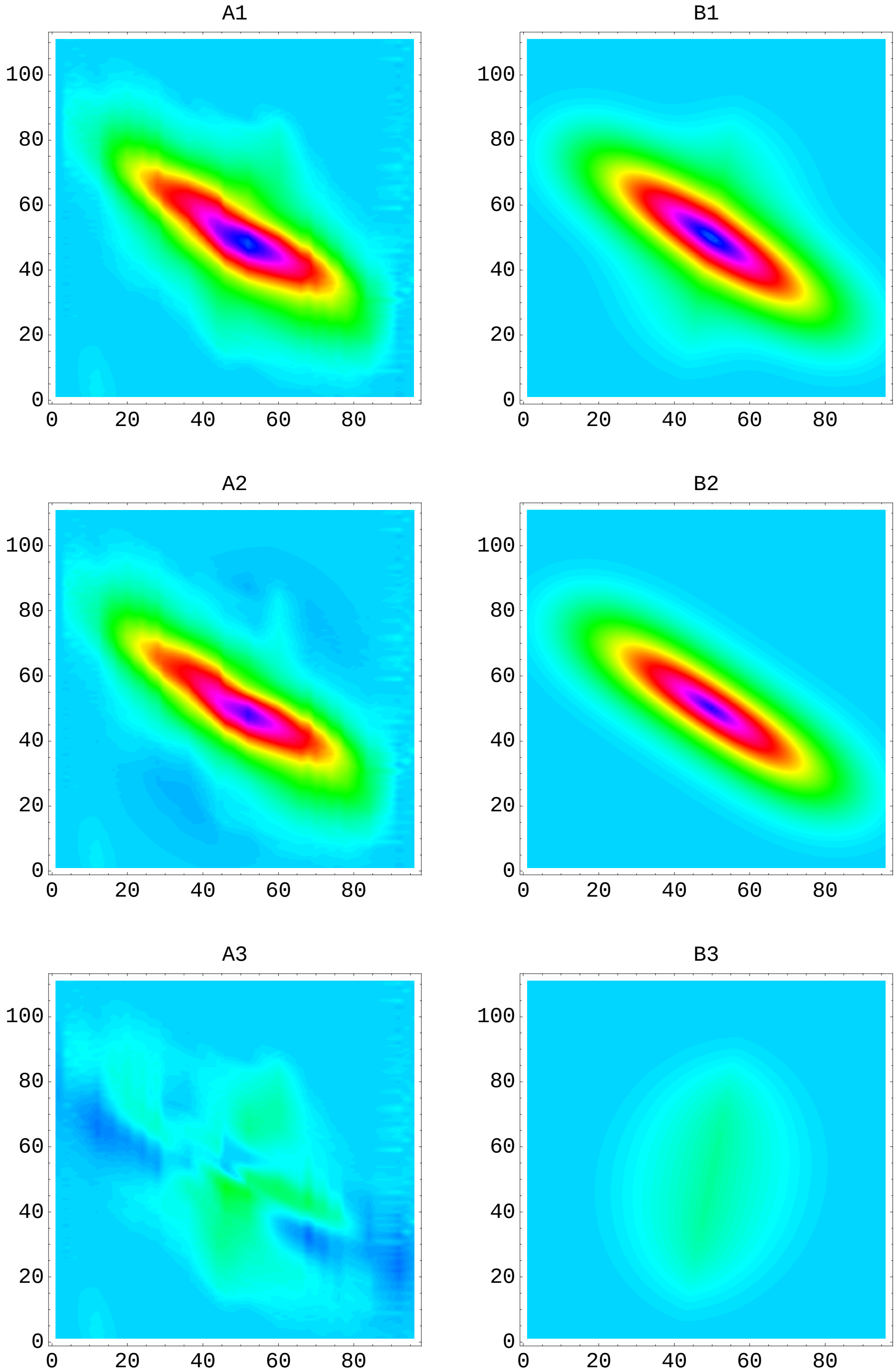

FIG. IV: PS1294.

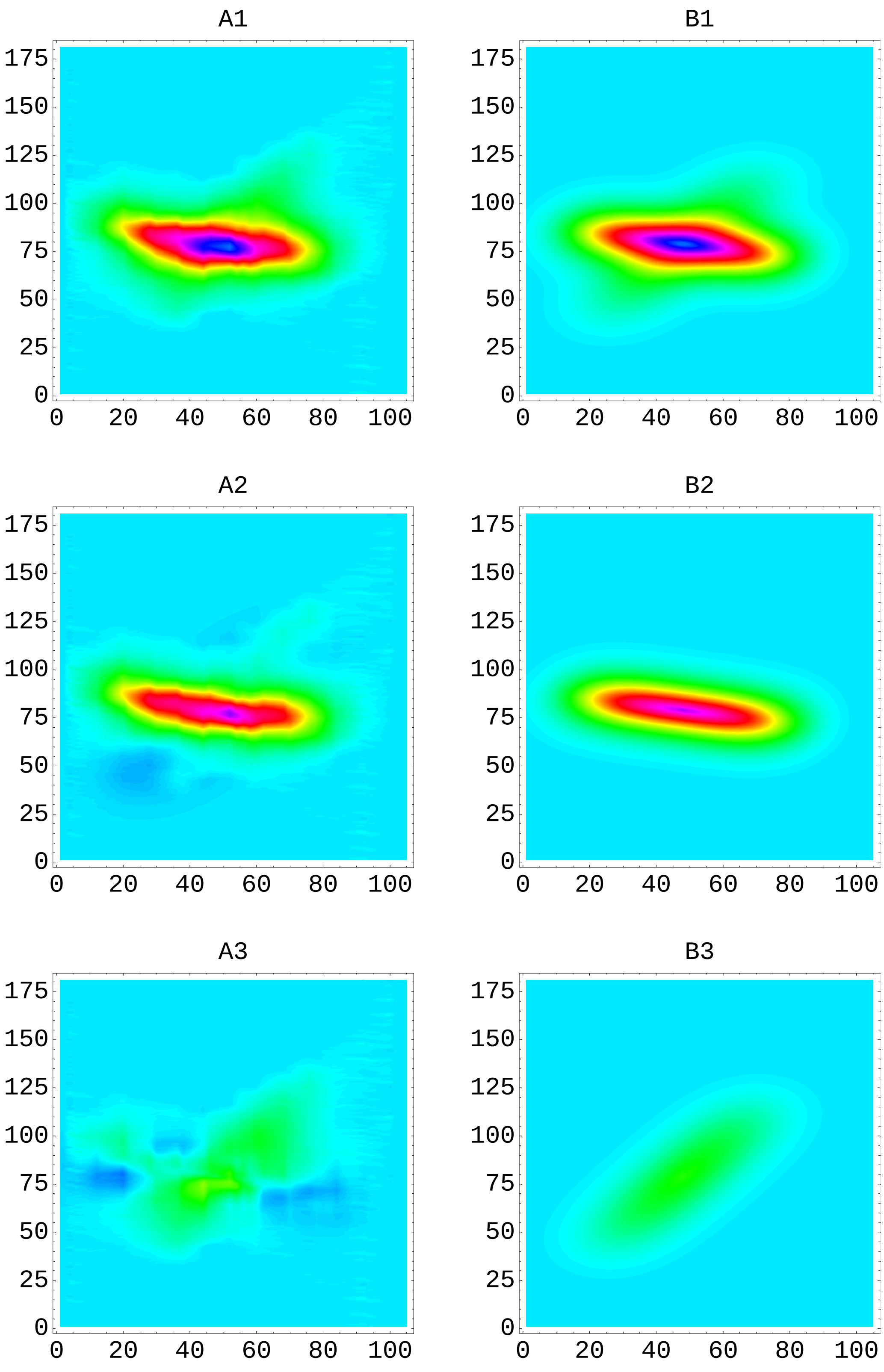

FIG. V: PS1426.

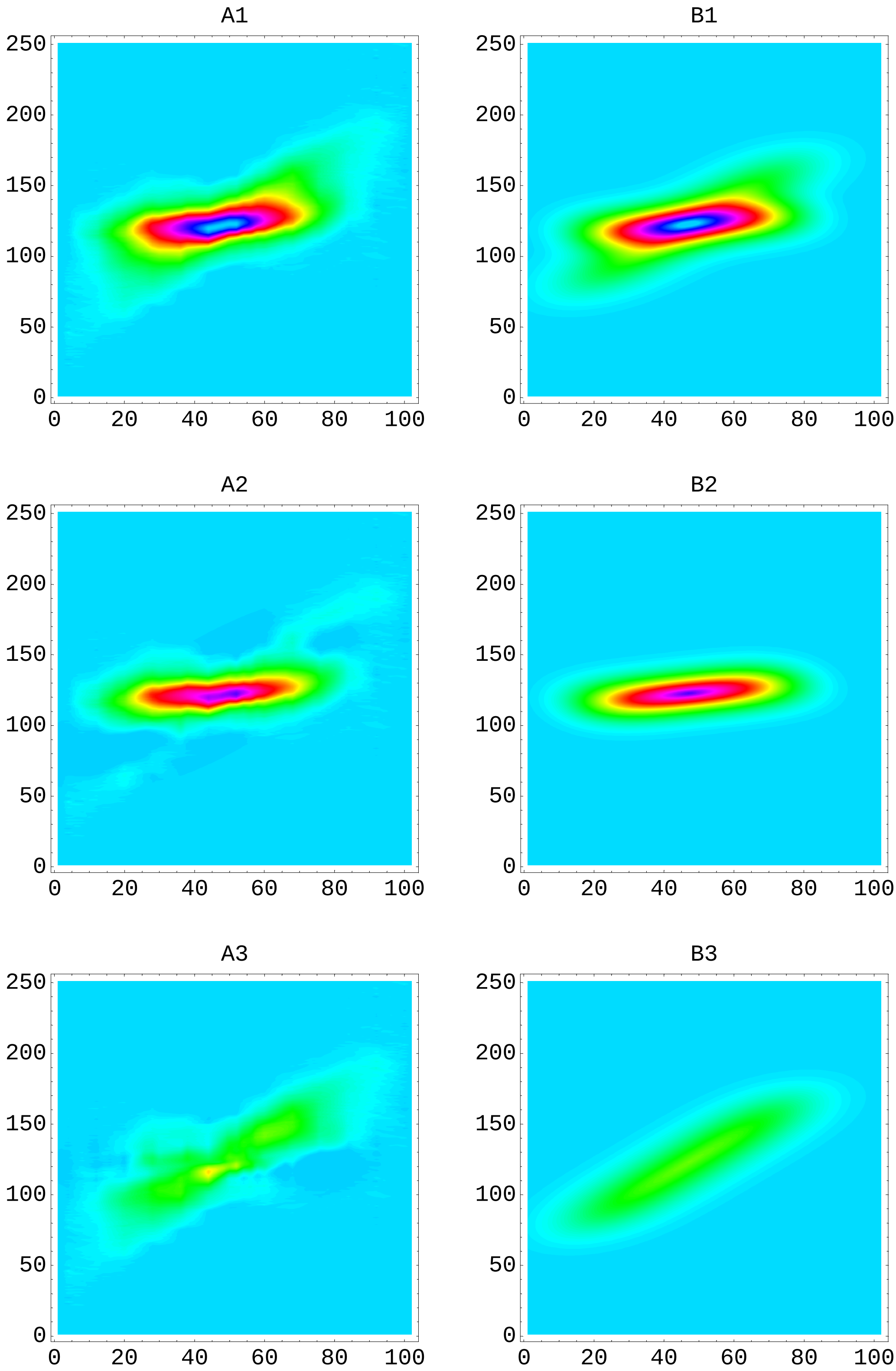

FIG. VI: PS1556.

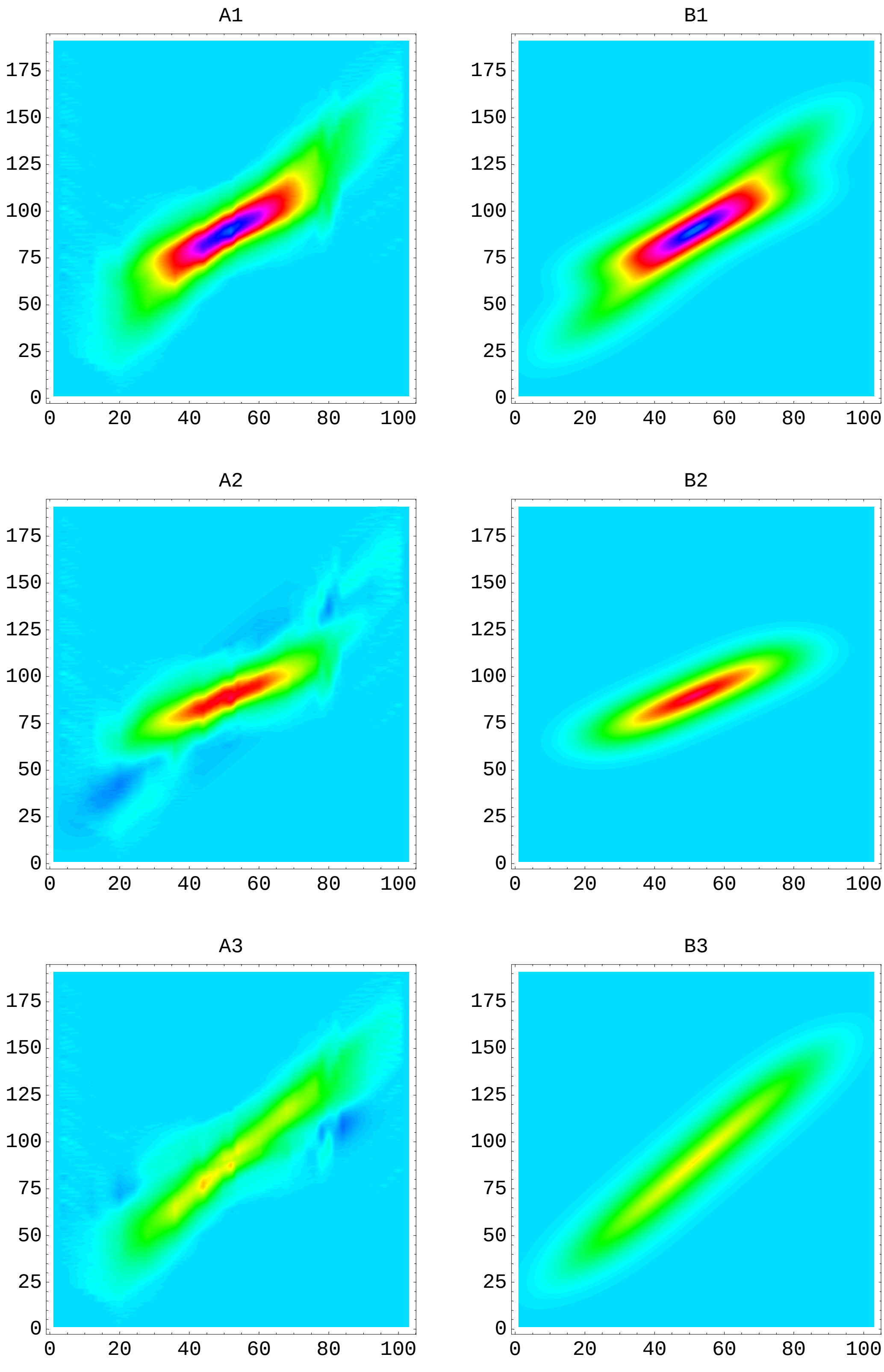

FIG. VII: PS1687.

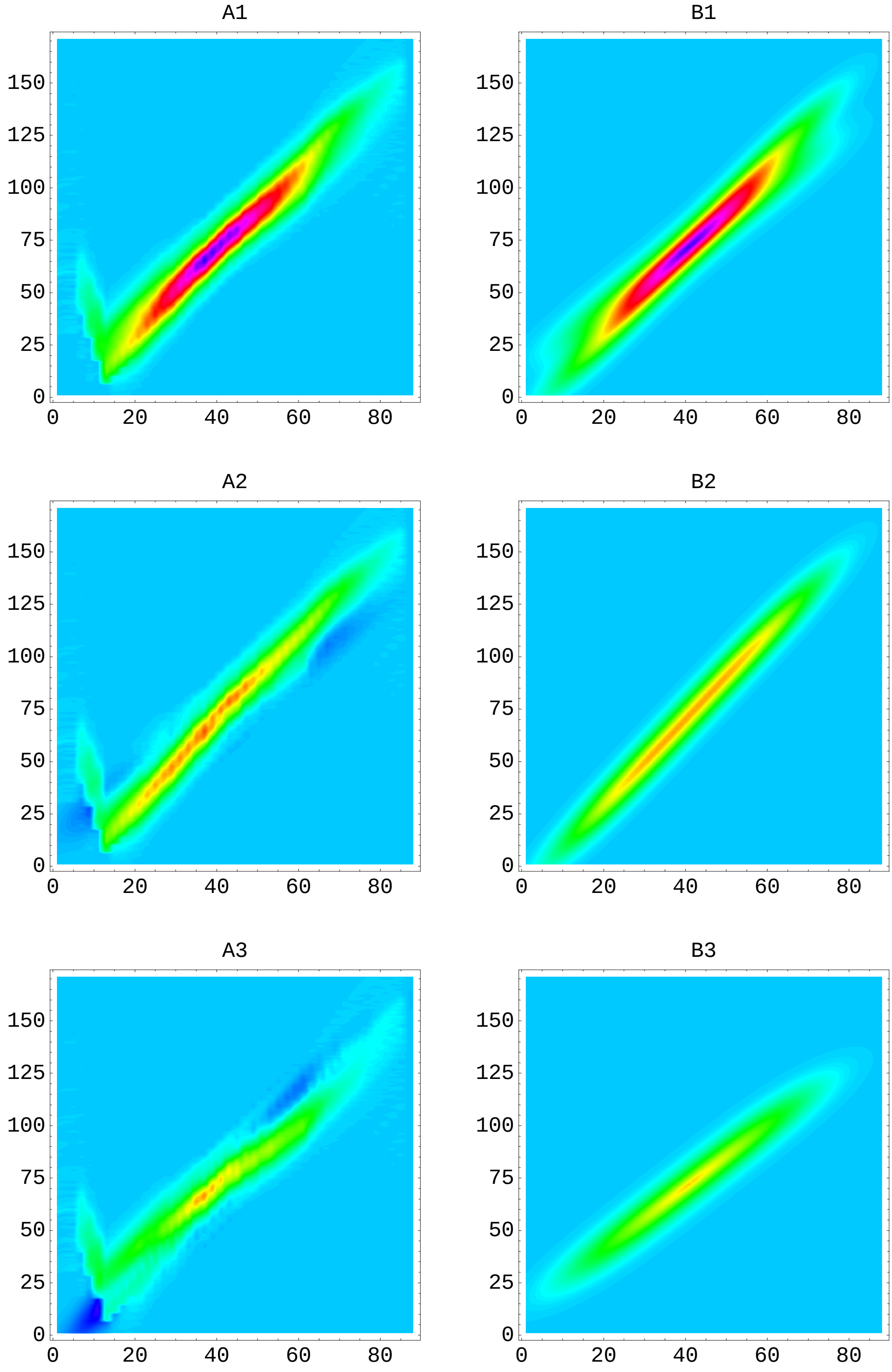

FIG. VIII: PS1948.

From the reconstructed PSs it is possible to get the emittance of portions of them: what we did was to cut a fixed percentage of charge from the secondary beam only, then recalculate the overall emittance of the whole charge left. It is also possible to find each beam's component emittance but, since we cannot control the charge content of main and secondary beam (see FIG. X), the data obtained are quite scattered and not comparable between themselves. Our results are shown in FIG. IX.

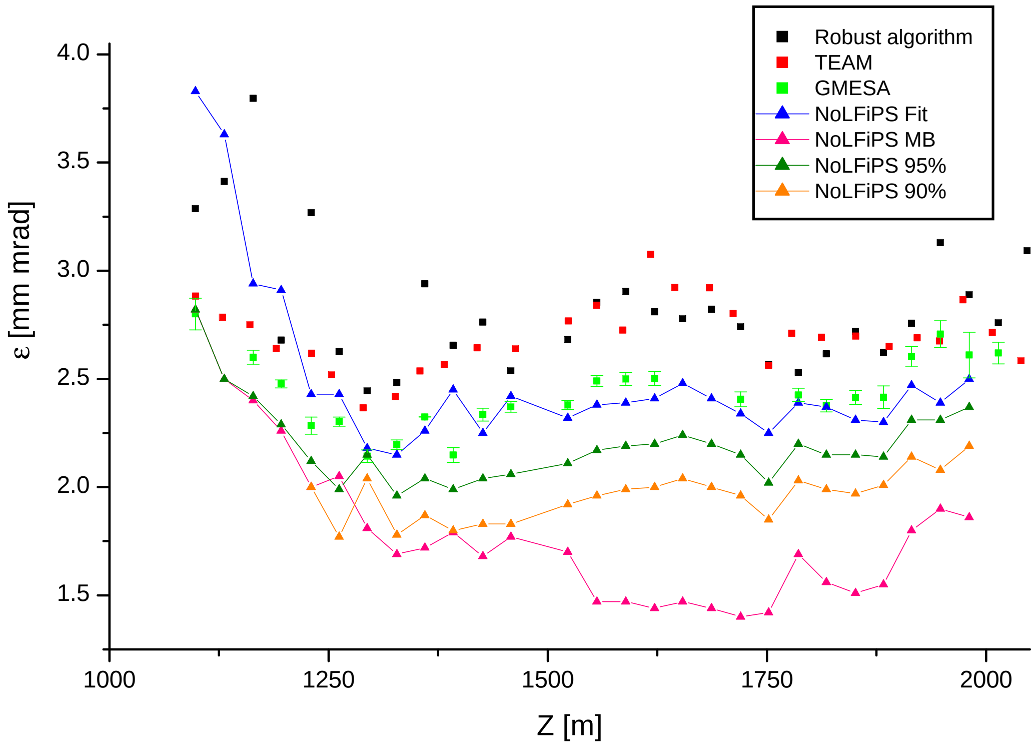

FIG. IX: Emittance values obtained from NoLFiPS compared with other codes, namely the Robust algorithm [4], TEAM [5] and GMESA [6]. Notice that the percentage of charge displayed by the dark green and orange data, is calculated on the reconstructed total charge (see FIG. X), NOT the nominal PS charge.

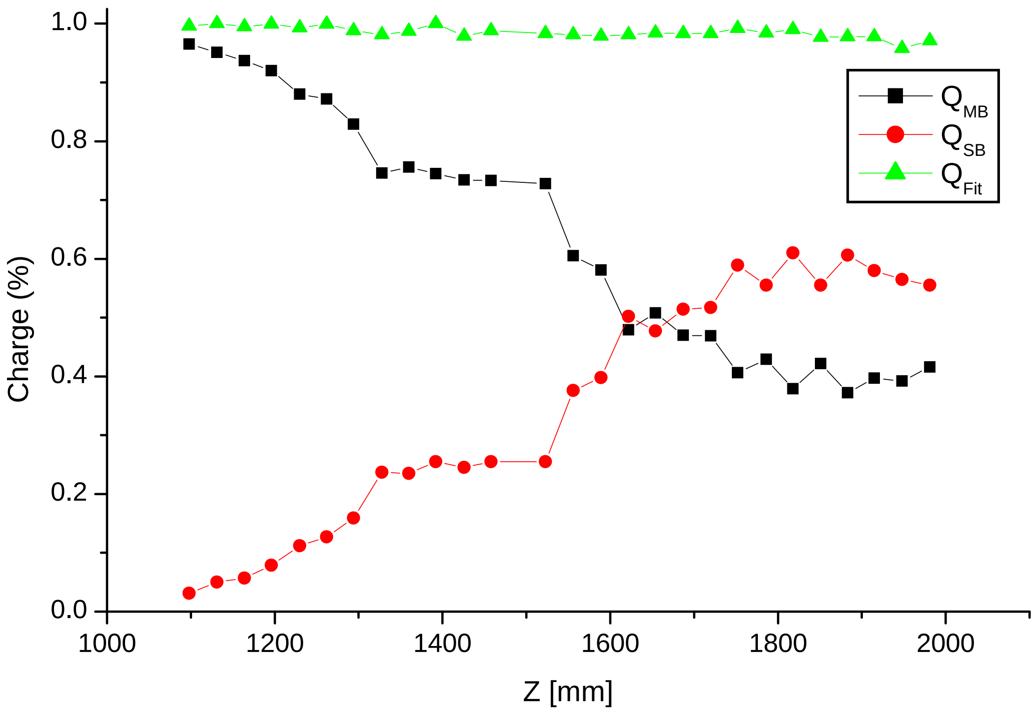

FIG. X: Charge values for the reconstructed PS and the two beam components. The MB and SB seem to swap. Notice that the two beam charges remain both close to 50% after the waist: this is due to fact that the core is better fitted by this configuration and represents a limit of the least squares method of fitting.

Acknowledgments

This work has been partially supported by the EU Commission in the Sixth Framework Program, Contract No. 011935, EUROFEL.

---

[1] J.D. Lawson, *The Physics of Charged-Particles Beams*, Clarendon Press, Oxford, 1988.

[2] L. Serafini and J.B. Rosenzweig, *Envelope analysis of intense relativistic quasi laminar beams in RF photoinjectors: a theory of emittance compensation*, Phys. Rev. E **55**, 7565 (1997).

[3] L. Catani et al., *Design and characterization of a movable emittance meter for low-energy electron beams*, Rev. Sci. Inst. **77**, 93301 (2006).

[4] D. Filippetto, Sparc Note SPARC/EBD-07/002

[5] A. Cianchi et al., Sparc Note SPARC/EBD-07/003

[6] A. Bacci, Sparc Note SPARC/EBD-07/004